NASA Technical Memorandum 87235

Role of Molybdenum in the Na_2SO_4 Induced Corrosion of Superalloys at High Temperature

A.K. Misra
Lewis Research Center
Cleveland, Ohio

Prepared for the
TMS-AIME Annual Meeting
New Orleans, Louisiana, March 2–6, 1986

NASA

ROLE OF MOLYBDENUM IN THE Na_2SO_4 INDUCED CORROSION OF SUPERALLOYS AT HIGH TEMPERATURE

A.K. Misra*
National Aeronautics and Space Administration
Lewis Research Center
Cleveland, Ohio 44135

E-2905

SUMMARY

Sodium sulfate induced corrosion of a molybdenum containing nickel-base superalloy, Udimet 700, have been studied in laboratory furnace tests and in a high velocity (Mach 0.3) burner rig. The effect of SO_2 content in the atmosphere on the corrosion behavior in the laboratory furnace tests has been determined. Catastrophic corrosion occurs only when the melt contains MoO_3 in addition to Na_2SO_4 and Na_2MoO_4. The conditions under which catastrophic corrosion occurs are identified and a mechanism is described to explain the catastrophic corrosion.

INTRODUCTION

Deposition of alkali sulfates on combustion turbine blades and vanes is known to cause accelerated corrosion of these components, and this is known as hot corrosion. Molybdenum containing nickel-base superalloys are extensively used as gas turbine blading materials and the primary role of Mo is to increase the strength of the alloy. Although the beneficial effect of Mo in increasing the strength of the alloy is well known, there is considerable controversy whether Mo is beneficial or detrimental for the hot corrosion resistance of the alloy. Catastrophic corrosion is observed for the Mo containing nickel-base superalloys in laboratory furnace tests in 1 atm O_2 (refs. 1 to 4). On the other hand, the burner rig tests do not always show the detrimental effect of Mo. Bergman et al. (ref. 5) and Hardt et al. (ref. 6) observed no detrimental effect of Mo at temperatures of the order of 871 to 915 °C; but at higher temperatures, e.g., 950 to 1040 °C, catastrophic corrosion was observed. However, Hardt et al. (ref. 6) have pointed out that catastrophic corrosion was not necessarily related to the Mo component of the alloys since the alloys without Mo also suffered from catastrophic corrosion at 1040 °C. Morrow et al. (ref. 7) have concluded that Mo was not harmful in the burner rig hot corrosion tests. Indeed, in the tests of Morrow et al. (ref. 7), the addition of Mo decreased the hot corrosion attack of some alloys. Burner rig tests in this laboratory in the past (refs. 8 to 10) also fail to show any detrimental effect due to the Mo component of the superalloys.

Goebel et al. (ref. 1) have postulated an acidic fluxing mechanism to explain the catastrophic corrosion of Mo containing alloys in laboratory furnace tests in 1 atm O_2. According to this mechanism addition of MoO_3 to the

---

*Case Western Reserve University, Dept. of Metallurgy and Materials Science, Cleveland, Ohio and NASA Resident Research Associate.

Na_2SO_4 melt lowers the Na_2O activity of the melt, thus making the melt more acid. The acidified melt then dissolves the protective oxides like Al_2O_3. Later Fryburg et al. (ref. 3), in their studies on the hot corrosion of B-1900, showed that catastrophic corrosion occurs by the conversion of Na_2SO_4 to Na_2MoO_4 and formation of a Na_2MoO_4-MoO_3 melt. Bourhis and St. John (ref. 11) have suggested that catastrophic corrosion occurs by the formation of a MoO_3 liquid layer at the scale-metal interface. The mechanisms described above are for an atmosphere containing O_2 only. The gas turbine atmosphere always contains small amounts of SO_2 and SO_3, the level depending on the fuel. There have been several studies on the effect of SO_2 plus SO_3 on the Na_2SO_4 induced corrosion of nickel-base alloys (refs. 12 to 14). Most of these studies except that of McKee et al. (ref. 12) were undertaken for alloys containing no Mo. Although the superalloys used in the study of McKee et al. (ref. 12) contained Mo, no particular effect of Mo on the hot corrosion process was described in their study.

This paper describes the hot corrosion of a Mo-containing nickel-base superalloy, Udimet 700 (composition in weight percent equals Cr 14.8, Co 17.5, Al 4.4, Ti 2.95, Mo 5.03, Ni balance). Laboratory furnace tests using both O_2 and O_2+SO_2+SO_3 atm and high velocity burner rig (Mach 0.3) tests are employed to study the hot corrosion of the superalloy. The conditions under which catastrophic corrosion occurs are identified and a mechanism is described to explain the catastrophic corrosion.

EXPERIMENTAL PROCEDURE

Laboratory Furnace Tests

The test samples were coupons approximately of size 23.5 by 10.8 by 2.3 mm with a hole in one end. All surfaces were glass bead blasted to give a uniform surface finish. The coupons were cleaned ultrasonically in trichloroethylene, detergent, distilled water, acetone, and alcohol, and then dried in an oven at 120 °C. The samples were coated with Na_2SO_4 by air-brushing a saturated solution of the salt onto the coupons, which were heated on a hot plate to about 200 °C. The corrosion experiments were performed in a vertical tube furnace and in flowing gas atmospheres containing either O_2 or O_2+SO_2+SO_3 mixture. For experiments with the O_2-SO_2-SO_3 mixture, a platinum catalyst was placed just beneath the corrosion sample in order to maintain SO_2-O_2-SO_3 equilibrium. Continuous gravimetric measurements were made with a microbalance. The temperature range of interest in the present study is 900 to 950 °C.

Burner Rig Tests

The details of the Mach 0.3 burner rig used in the present study have been described in several other publications (refs. 15 and 16), and only a brief description will be given here. Jet A-1 fuel (sulfur content of about 0.05 wt %) and preheated air are mixed and ignited in the burner and the combustion products exit through a L605 (cobalt-base superalloy) nozzle. The salt solution is pumped into the combustor by a peristaltic pump at a calibrated flow rate of 200 cc/hr. The solution is air atomised into a fine spray, the atomising pressure being of the order of 30 psi. The concentration of Na in the flame is varied by changing the concentration of the salt solution. The

corroding sample is a cylinder with o.d. of 1.9 cm and a height of 1.3 cm, and the sample is spring loaded in between two ceramic (Al_2O_3) spacers. The entire sample assembly is rotated at about 200 rpm , and the size of the sample is such that all of the sample is immersed in the combustion flame. This assumes uniform temperature as well as uniform salt deposition throughout the sample. All the corrosion experiments were conducted at 900 °C, and each corrosion cycle consisted of 2 hr at temperature followed by cooling to ambient temperature.

RESULTS AND DISCUSSION

Corrosion in Laboratory Furnace Tests in 1 atm O_2

The corrosion kinetics, in general, can be divided into three distinct periods, which is schematically shown in figure 1. The three different periods in the kinetics are: (a) an initial period, during which there is rapid increase in the weight of the sample, (b) induction period, and (c) period of accelerated corrosion, during which large weight gains are observed and the corrosion is catastrophic. The length of each period in the corrosion kinetics and the total weight gain or the extent of corrosion during each period are strong functions of the amount of Na_2SO_4 and temperature. In some cases, the length of the initial period was 2 to 3 hr, whereas, in other cases, the length of the initial period was 40 to 50 hr. Similarly, the length of the induction period in some cases was 2 to 3 hr, whereas in other cases, it was 200 to 300 hr. The length of the induction period was observed to be very small for smaller coating thicknesses; for example, at 950 °C, no induction period was observed for a salt coating of 0.5 mg/cm^2, as compared to an induction period of 60 to 70 hr for a salt coating of 3.5 mg/cm^2. Similarly, the length of the induction period increases considerably with a decrease of temperature, e.g., the length of the induction period for a coating of 3.5 mg/cm^2 was observed to be 200 hr at 900 °C, as compared to 60 to 70 hr at 950 °C.

The test samples, corroded for different lengths of time, were washed with hot distilled water, and the resulting solutions were analyzed for various water soluble species like Na, Cr, $SO_4^{=}$, Mo, Ni, and Co. No significant amounts of Ni and Co were detected in the waterwashed solution. Figure 2 shows the amount of various species in millimoles as a function of time for U-700, coated with two different amounts of Na_2SO_4 (3.5 and 0.5 mg/cm^2), and corroded at 950 °C. The corresponding corrosion kinetics are also shown in figure 2. The important feature of the results of the chemical analysis is that the beginning of the period of accelerated corrosion is marked by a rapid rise in the Mo content of the waterwashed solution. The $SO_4^{=}$ and Mo in the solution are due to the presence of Na_2SO_4 and Na_2MoO_4+MoO_3, respectively. The Cr in the solution is primarily due to the presence of Na_2CrO_4. Evidence of this could be obtained from the yellowish deposit on the sample, which was identified by x-ray diffraction to be Na_2CrO_4. The Na in the solution is due to Na_2SO_4, Na_2CrO_4, and Na_2MoO_4. The compounds, Na_2CrO_4, Na_2MoO_4, Na_2SO_4, and MoO_3 have melting points below 900 °C (ref. 17), and, therefore, at temperature, these compounds would have existed as a melt. The melt at any point during corrosion would be a mixture of Na_2SO_4-Na_2CrO_4-Na_2MoO_4-MoO_3, and from the chemical analysis of the various species, the chemical composition of the melt at a given time can be obtained, which is described as follows: From stoichiometry:

$$\frac{1}{2}\,\eta_{Na} = \eta_{Na_2SO_4} + \eta_{Na_2CrO_4} + \eta_{Na_2MoO_4} \quad (1)$$

$$\eta_{Mo} = \eta_{Na_2MoO_4} + \eta_{MoO_3} \quad (2)$$

$$\eta_{Cr} = \eta_{Na_2CrO_4} \quad (3)$$

$$\eta_{SO_4^{=}} = \eta_{Na_2SO_4} \quad (4)$$

where η_x gives the number of moles of the species x in the waterwashed solution. From the solution of equations (1) to (4), the number of moles of Na_2SO_4, Na_2CrO_4, Na_2MoO_4, and MoO_3 in the melt can be obtained. Table I shows the mole fraction of various components in the melt as a function of time for U-700, coated with 3.5 mg/cm^2 Na_2SO_4, and corroded at 950 °C. From table I, it is seen that the melt composition changed with time. The melt was Na_2SO_4 at the beginning, Na_2SO_4-Na_2CrO_4 containing small amount of Na_2MoO_4 during the initial period, Na_2CrO_4-Na_2MoO_4 during the induction period, Na_2CrO_4-Na_2MoO_4-MoO_3 containing small amount of Na_2SO_4 at the beginning of the period of accelerated corrosion, and Na_2MoO_4-MoO_3 containing small amount of Na_2SO_4 and Na_2CrO_4 at a later time during the period of accelerated corrosion. Only Na and Mo were detected in the waterwashed solution during the period of accelerated corrosion for a coating of 0.5 mg/cm^2 (fig. 2(b)). From stoichiometry the chemical composition of the melt after 5 hr of corrosion for a coating of 0.5 mg/cm^2 Na_2SO_4 was determined to be Na_2MoO_4-59 mole percent MoO_3.

From the results of the chemical analysis it becomes apparent that all or most of the Na_2SO_4 are converted to Na_2MoO_4 during the course of corrosion. Therefore, it would be instructive to examine the corrosion of Na_2MoO_4 coated samples. The corrosion kinetics for the Na_2MoO_4 coated sample and the results of the chemical analysis are shown in figure 3. An induction period is observed before the onset of accelerated corrosion, and the chemical analysis shows that the onset of accelerated corrosion is marked by a rapid increase in the Mo content of the melt. Because the composition of the melt was Na_2MoO_4 to begin with, the increase in the Mo content of the melt must be due to the addition of MoO_3 to the melt. It appears that the end of the induction period is associated with the addition of certain amount of MoO_3 to the Na_2MoO_4 melt. To further confirm the role of MoO_3 in inducing catastrophic corrosion, additional experiments were conducted in which a slurry of MoO_3 was airbrushed onto the sample, and above this, a Na_2MoO_4 layer was applied by airbrushing. The mixture applied corresponds to Na_2MoO_4-23 mole percent MoO_3. The kinetics of corrosion by the Na_2MoO_4-MoO_3 melt are shown in figure 4. For comparison, the weight gain data for Na_2MoO_4 only are also presented in figure 4. It can be seen from figure 4 that when MoO_3 was added to the Na_2MoO_4 melt, the length of the induction period decreased considerably. These results further demonstrate that the melt must contain some MoO_3 in addition to Na_2MoO_4 for the catastrophic corrosion to occur.

MoO_3 is highly volatile; for example, the equilibrium vapor pressure of MoO_3 at 900 °C is of the order of 0.05 atm. Thus, any MoO_3 formed can

evaporate instantaneously; however, the evaporation studies by the present author (ref. 18) have shown that the rate of evaporation of MoO_3 is considerably decreased when dissolved in Na_2MoO_4. The rates of evaporation of Na_2MoO_4, MoO_3, and Na_2MoO_4-MoO_3 melts with different MoO_3 concentrations at 900 °C are shown in table II. From table II, it is clearly seen that the rate of evaporation of MoO_3 is considerably decreased when dissolved in Na_2MoO_4; for example, a comparison of the rate of evaporation of MoO_3 at $x_{MoO_3} = 0.4$ with that at unit activity shows that the rate of evaporation is decreased by a factor of 10^{-3}. Thus, the principal role of Na_2MoO_4 appears to be to stabilize the MoO_3 in the melt by decreasing the equilibrium vapor pressure of MoO_3.

A typical scale morphology for the corrosion beneath a Na_2MoO_4-MoO_3 melt is shown in figure 5. A pitting type of corrosion morphology is evident from figure 5, and the pit is seen to be Mo rich. Ni and Cr are also present inside the pit. A thick, porous oxide layer can be seen above the pit. The porous oxide layer consists of primarily NiO and Cr_2O_3. The detailed examination of the pit at a higher magnification (fig. 6) shows abundance of Ni, Na, Mo, and Cr throughout the pit. Ni and Mo appear to be uniformly distributed throughout the pit, whereas, Cr is present as discrete particles in the pit. The pit is seen to be in direct contact with the underlying alloy. No Cr depletion is observed in the alloy regions beneath the pit. The x-ray maps in figures 5 and 6 show only the important elements; the other elements like Co, Al, and Ti are present in small amounts and x-ray maps for these elements are not shown in order to maintain simplicity and emphasize the primary constituents. Co is usually observed to be present along with Ni..

Corrosion in Laboratory Furnace Tests in O_2-SO_2-SO_3 Atmosphere

The corrosion kinetics for U-700, coated with 0.7 mg/cm^2 Na_2SO_4, and oxidized in O_2 plus 0.108 percent SO_2-SO_3 at 950 °C is shown in figure 7. The alloy corrodes at a slower rate during the first 10 to 15 hr, which may be called the induction period, after which the rate gradually starts to increase until it becomes linear. The rate of corrosion during the linear period is considerably higher (of the order of 4 to 5 mg/cm^2-hr), and the corrosion can be termed as catastrophic. In general, the corrosion kinetics can be divided into an induction period and a final period of catastrophic corrosion with a transition period in between. The results of the chemical analysis for the corrosion of U-700 in O_2+0.18 percent SO_2-SO_3 are shown in table III. During the period of catastrophic corrosion the melt at all times consists of MoO_3 in addition to Na_2SO_4 and Na_2MoO_4, whereas, during the induction period only Na_2SO_4 is present. It appears that the melt must contain MoO_3 in addition to Na_2SO_4 and Na_2MoO_4 for the catastrophic corrosion to occur, which is also very similar to that of corrosion in an atmosphere containing O_2 only. The critical role of MoO_3 in inducing catastrophic corrosion of U-700 in O_2-SO_2-SO_3 atm can be elucidated from the corrosion experiments in which a Na_2MoO_4-coated sample is oxidized in O_2+SO_2+SO_3 atm, as explained below. The oxidation of a Na_2MoO_4-coated sample in O_2+SO_2+SO_3 atm would generate MoO_3 along with Na_2SO_4 from the beginning because of the reaction:

$$Na_2MoO_4(\ell) + SO_3(g) = Na_2SO_4(\ell) + MoO_3(\ell) \qquad (5)$$

To confirm that MoO_3 can be obtained by the reaction of Na_2MoO_4 and SO_3, a Pt coupon was coated with about 7.6 mg of Na_2MoO_4 and exposed to O_2 plus 0.108 percent SO_2-SO_3 at 950 °C, and after 4 hr of exposure, the coupon was washed in distilled water and the solution was analyzed for Na, $SO_4^{=}$, Mo. From the results of the chemical analysis and from equations (1) to (4), the composition of the melt is obtained to be $n_{Na_2MoO_4}$ = 0.0194 mM, $n_{Na_2SO_4}$ = 0.0176 mM, n_{MoO_3} = 0.0168 mM (mM represents millimoles.) Thus the critical role of MoO_3 in inducing catastrophic corrosion can be confirmed, if no induction period is observed for the corrosion of the Na_2MoO_4-coated sample in O_2+SO_2+SO_3 atmosphere. Figure 8 shows the corrosion kinetics for the Na_2MoO_4-coated sample in O_2 and O_2+0.108 percent SO_2-SO_3 atm; and indeed, no induction period is observed for corrosion in O_2+0.108 percent SO_2-SO_3 atm as compared to a long induction period for corrosion in 1 atm O_2. This clearly demonstrates the critical role of MoO_3 in inducing catastrophic corrosion of the alloy.

A porous scale is developed during the period of catastrophic corrosion in O_2 plus 0.108 percent SO_2-SO_3, and a significant portion of the scale spalled during cooling. The scale morphology (fig. 9) shows a porous outer scale and internal sulfides in the alloy. Also, a Mo-rich layer is observed at the scale-metal interface.

The effect of SO_2 plus SO_3 concentration in the atmosphere on the corrosion kinetics is shown in figure 10. For O_2 plus 105 ppm SO_2-SO_3, catastrophic corrosion is observed after an induction period, and a pitting type of morphology (fig. 11) is observed during the period of catastrophic corrosion, the pit being Mo-rich. This type of morphology is very similar to that obtained in an atmosphere containing O_2 only. The scale morphology for corrosion in O_2+0.24 percent SO_2-SO_3 was observed to be very similar to that of O_2+0.108 percent SO_2-SO_3; however, the rate of corrosion in O_2+ 0.24 percent SO_2-SO_3 was observed to be lower than that in the atmosphere containing 0.108 percent SO_2+SO_3. From figure 10 it is seen that catastrophic corrosion is not observed in atmospheres containing 1 and 2 percent SO_2 plus SO_3, and the rate of corrosion is considerably lower (of the order of 0.18 to 0.2 mg/cm^2-hr); however, the rate is still higher than that of pure oxidation. For example, the weight gain for U-700 after oxidation in air for 90 hr at 950 °C is only of the order of 1.5 to 2 mg/cm^2. The scale morphology for corrosion in O_2 plus 1 percent SO_2-SO_3 and O_2 plus 2 percent SO_2-SO_3 (fig. 12) shows considerable internal attack with an internal sulfidation zone ahead of an internal oxidation zone. This type of morphology is typical of a sulfidation-oxidation type of attack as observed by several investigators (refs. 20 and 21). The chemical analysis of the waterwashed solution of the corroded samples as a function of the SO_2+ SO_3 content of the atmosphere is shown in table IV as mole fraction of various components, e.g., Na_2SO_4, MoO_3, and Na_2MoO_4. An increase in the SO_2+SO_3 content of the atmosphere leads to a decrease in the mole fraction of Na_2MoO_4 and MoO_3 in the melt. It is interesting to note that no Mo could be detected in the water washed solution for corrosion in O_2 plus 1 percent and O_2+2 percent SO_2-SO_3 atmospheres.

Mechanism of Corrosion by Na_2MoO_4-MoO_3 and Na_2SO_4-Na_2MoO_4-MoO_3 Melts

Based on transport considerations and Rapp-Goto criterion for fluxing (ref. 22), a corrosion mechanism has been proposed by the present author (refs. 18 and 19). It is suggested that Mo exists in the melt as Mo^{+4} and Mo^{+6} (or equivalently dissolved MoO_2 and MoO_3). The equilibrium between dissolved MoO_2 and MoO_3 in the melt can be described by the reaction:

$$\underline{MoO_2} + \frac{1}{2} O_2 = \underline{MoO_3} \qquad (6)$$

Since the P_{O_2} at the melt-gas interface is higher than the melt-alloy interface, the concentration of MoO_3 would be greater at the melt-gas interface and the concentration of MoO_2 would be greater at the melt-alloy/-oxide interface. This would result in migration of MoO_3 inward from the melt-gas to the melt-oxide/alloy interface and migration of MoO_2 outward from the melt-oxide/alloy interface. The schematics of the formation of MoO_3 at the melt-gas interface and various gradients across the melt are shown in figure 13. Based on the existence of Mo as Mo^{+4} plus Mo^{+6} and possible electronic conductivity for the MoO_3 containing melts, a corrosion mechanism is proposed in which Ni dissolves as Ni^{++} at the melt-alloy/-oxide interface and NiO is formed at the melt-gas interface. The transport of Ni^{++} through the melt is suggested to occur in conjunction with electron conduction in the melt, the electron conduction arising due to the MoO_3 component of the melt. The schematics of the suggested mechanism is shown in figure 14.

Corrosion in High Velocity (Mach 0.3) Burner Rig Tests

The weight change data for the burner rig tests for two Na levels (1 and 3 wppm) are shown in figure 15. The alloy loses weight at a steady rate from the beginning, and after certain time period (100 hr for 1 wppm, 60 hr for 3 wppm), the alloy starts to gain weight. For 3 wppm Na, the rate of weight gain during the weight gain period was observed to be very high, e.g., of the order of 22 mg/hr. The scale morphology during the period of constant weight loss, illustrated in figure 16, shows a thin external scale and an internal penetration zone consisting of small sulfide particles. The internal penetration zone is depleted of Cr. During the period of weight loss the corrosion proceeds by the increase in the depth of the internal penetration zone. The scale morphology after the occurrence of rapid weight gain shows severe corrosion and extensive sulfidation, which is illustrated in figure 17. The corrosion occurs mostly by internal penetration, as was evidenced by the presence of metallic regions in the scale. A sulfide network is observed beneath a thick internal oxide region; this type of morphology suggests a sulfidation-oxidation type of mechanism (refs. 20 and 21) in which rapid oxidation occurs due to preferential oxidation of the sulfides. The total depth of internal penetration in figure 17 is observed to be of the order of 1.5 mm, and therefore, the corrosion can be termed as catastrophic. Although the alloy suffers from catastrophic corrosion, the morphology of corrosion is entirely different from that obtained in the laboratory furnace tests during the period of catastrophic corrosion. In the laboratory furnace tests accelerated corrosion occurs by the formation of a porous oxide layer above a Mo rich melt as compared to heavy sulfidation observed in the burner rig tests.

The results of the chemical analysis for corrosion in the burner rig are shown in table V. The amount of Na_2SO_4 on the corroding sample during the period of weight loss is very small, the maximum being of the order of 0.3 mg/cm^2. There is a significant increase in the amount of Na_2SO_4 and other Na compounds e.g., Na_2CrO_4 and Na_2MoO_4, during the period of weight gain. The increase in the amount of salt deposit on the corroding sample during the weight gain period can be attributed to the development of a thick scale, which helps in retaining the salt in the oxide. Significant quantities of Mo are detected in the waterwashed solution during the period of rapid weight gain; however, from stoichiometry, all of the Mo is observed to be present as Na_2MoO_4. The melt does not contain any MoO_3 during the period of weight gain, and this probably explains why the typical scale morphology for corrosion by the MoO_3 containing melts was not produced in the burner rig tests.

Conditions for Catastrophic Corrosion Due to The Mo Component of The Alloy

The present study has shown that the melt must contain MoO_3 in addition to Na_2SO_4 and Na_2MoO_4 for the catastrophic corrosion to occur; formation of Na_2MoO_4 only does not result in catastrophic corrosion. In the laboratory furnace tests in 1 atm O_2 a Na_2MoO_4-MoO_3 melt is formed and catastrophic corrosion occurs. On the other hand, in the laboratory furnace tests using O_2-SO_2-SO_3 atm, a MoO_3 containing melt is formed only for the lower SO_2 containing atmospheres. Chemical analysis showed that the stability of MoO_3 decreases and that of Na_2SO_4 increases with an increase in P_{SO_2} in the atmosphere. At 950 °C, for SO_2 content greater than 1 percent, Na_2SO_4 was observed to be the most stable melt, and no Mo could be detected in the melt. The relative stability of Na_2SO_4, Na_2MoO_4, and MoO_3 are governed by the equilibria for reaction 5. From thermodynamic considerations, it can be derived that at lower temperatures, Na_2SO_4 would be the most stable melt even for lower SO_2 contents in the atmosphere. Thus, for many low temperature applications in which the turbine atmosphere contains significant amount of SO_2, e.g., marine gas turbine and many industrial gas turbines, the Mo component of the alloy might not be detrimental for the hot corrosion resistance. In the burner rig tests, although Mo is detected in the melt, all of the Mo is observed to be in the form of Na_2MoO_4. This is due to two reasons. First, although the rate of evaporation of MoO_3 in the laboratory furnace tests is considerably reduced then dissolved in Na_2MoO_4, the rate evaporation may be higher in the high velocity environment of the burner rig. Second, according to the proposed corrosion mechanism (fig. 13) MoO_3 is formed at the melt-gas interface. In the burner rigs there is continuous deposition of Na_2SO_4 at this interface, and any MoO_3 formed would react with Na_2SO_4 to form Na_2MoO_4 and SO_3. Thus the melt would contain Na_2MoO_4 in addition to Na_2SO_4, but not any MoO_3. In the burner rig tests catastrophic corrosion is observed due to severe internal sulfidation; however, this is not due to the Mo component of the alloy since severe sulfidation can also be produced for alloys containing no Mo. From the above discussions it can be concluded that catastrophic corrosion due to the Mo component of the superalloy occurs only in limited situations.

REFERENCES

1. Goebel, J.A.; Pettit, F.S.; and Goward, G.W.: Mechanisms for the Hot Corrosion of Nickel-Base Alloys. Metall. Trans., vol. 4, no. 1, Jan. 1973, pp. 261-278.

2. Bornstein, N.S.; and Decrescente, M.A.: The Role of Sodium in the Accelerated Oxidation Phenomenon Termed Sulfidation. Metall. Trans, vol. 2, no. 10, Oct. 1971, pp. 2875-2883.

3. Fryburg, G.C.; Kohl, F.J.; Stearns, C.A.; and Fielder, W.L.: Chemical Reactions Involved in the Initiation of Hot Corrosion of B-1900 and NASA-TRW VIA. J. Electrochem. Soc., vol. 129, no. 3, Mar. 1982, pp. 571-585.

4. Peters, K.R.; Whittle, D.P.; and Stringer, J.: Oxidation and Hot Corrosion of Nickel-Based Alloys Containing Molybdenum. Corros. Sci., vol. 16, no. 11, 1976, pp. 791-804.

5. Bergman, P.A.; Sims, C.T.; and Beltran, A.N.: Development of Hot-Corrosion-Resistant Alloys for Marine Gas Turbine Service. Hot Corrosion Problems Associated with Gas Turbines, ASTM STP-421, ASTM, 1967, pp. 38-59.

6. Hardt, R.W.; Gambino, J.R.; and Bergman, P.A.: Marine Hot Corrosion Mechanism Studies. Hot Corrosion Problems Associated With Gas Turbines, ASTM STP-421, ASTM, 1967, pp. 64-84.

7. Morrow, H., III; Sponseller, D.L.; and Kelns, E.: The Effects of Molybdenum and Aluminum on the Hot Corrosion (Sulfidation) Behavior of Experimental Nickel-Base Superalloy. Metall. Trans., vol. 5, no. 3, Mar. 1974, pp. 673-683.

8. Santaro, G.J.: Hot Corrosion of Four Superalloys: HA-188, S-57, In-617 and TD-NiCrAL. Oxid. Met., vol. 13, no. 5, Oct. 1979, pp. 405-435.

9. Lowell, C.E.; Sidik, S.M.; and Deadmore, D.L.: Effect of Sodium, Potassium, Magnesium, Calcium, and Chlorine on the High Temperature Corrosion of IN-100, U-700, IN-792, and Mar.M-509. J. Eng. Power Trans., vol. 103, no. 2, Apr. 1981, pp. 294-307.

10. Lowell, C.E.; and Deadmore, D.L.: The Kinetics of High Velocity High Temperature Corrosion of U-700. Corrosion in Fossil Fuel Systems, I.G. Wright, ed., Electrochemical Society, 1983, pp. 365-394.

11. Bourhis, Y.; and Saint-John, C.: On the Role of Refractory Elements in the Hot Corrosion of Nickel-Base Alloys. Properties of High Temperature Alloys, Z.A. Foroulis and F.S. Pettit, eds., Electrochemical Society, 1977, pp. 595-606.

12. McKee, D.W.; Shores, D.A.; and Luthra, K.L.: The Effect of SO_2 and NaCl on High Temperature Hot Corrosion. J. Electrochem. Soc., vol. 125, no. 3, Mar. 1978, pp. 411-419.

13. Luthra, K.L.; Shores, D.A.: Mechanism of Na_2SO_4 Induced Corrosion at 600°-900° C. J. Electrochem. Soc., vol. 127, no. 10, Oct. 1980, pp. 2202-2210.

14. Chiang, K.T.; Pettit, F.S.; and Meier, G.H.: Low Temperature Hot Corrosion. High Temperature Corrosion, R.A. Rapp, ed., NACE publication, 1983, pp. 519-530.

15. Kohl, F.J., et al: Theoretical and Experimental Studies of the deposition of Na_2SO_4 from Seeded Combustion Gases. J. Electrochem. Soc., vol. 126, no. 6, June 1979, pp. 1054-1061.

16. Santoro, G.J., et al: Experimental and Theoretical Deposition Rates From Salt-Seeded Combustion Gases of a Mach 0-3 Burner Rig. NASA TP-2225, 1984.

17. Weast, R.C., ed.: CRC Handbook of Chemistry and Physics, 59th ed., CRC Press Inc., Boca Raton, FL, 1978-79.

18. Misra, A.K.: Mechanism of Na_2SO_4 Induced Corrosion of Molybdenum Containing Nickel Base Superalloys at High Temperatures I. Corrosion in Atmospheres Containing O_2 only. To be published in J. Electrochem. Soc., 1986.

19. Misra, A.K.: Mechanism of Na_2SO_4 Induced Corrosion of Molybdenum Containing Nickel Base Superalloys at High Temperatures II. Corrosion in O_2+SO_2 Atmospheres. To be published in J. Electrochem. Soc., 1986.

20. Spengler, C.J.; and Viswanathan, R.: Effect of Sequential Sulfidation and Oxidation on the Propagation of Sulfur in an 85 NI-15cr Alloy. Metall. Trans., vol. 3, no. 1, Jan. 1972, pp. 161-166.

21. Goebel, J.A.; and Pettit, F.S.: The Influence of Sulfides on the Oxidation Behavior of Nickel-Base Alloy. Metall. Trans., vol. 1, no. 12, Dec. 1970, pp. 3421-3429.

22. Rapp, R.A.; Goto, K.S.: The Hot Corrosion of Metal by Molten Salts. Proceedings of the Second International Symposium on Molten Salts, J. Braunstein and J.R. Selman, eds., Electrochemical Society, 1981, pp. 159-171.

TABLE I. - MOLE FRACTIONS OF VARIOUS COMPONENTS IN THE MELT AS A FUNCTION OF TIME FOR U-700, COATED WITH 3.5 mg/cm^2 Na_2SO_4, AND OXIDIZED AT 950 °C

[$X_{Na_2SO_4}$, $X_{Na_2CrO_4}$, $X_{Na_2MoO_4}$, and X_{MoO_3} are the mole fractions of Na_2SO_4, Na_2CrO_4, Na_2MoO_4, and MoO_3 in the melt, respectively.]

Time, hr	$X_{Na_2SO_4}$	$X_{Na_2CrO_4}$	$X_{Na_2MoO_4}$	X_{MoO_3}
0	1	-----	-----	-----
0.75	0.833	0.151	0.015	-----
3	.709	.237	.052	-----
7	.307	.614	.077	-----
15	.01	.846	.143	-----
50	-----	.694	.306	-----
60	.018	.478	.355	0.147
93	.032	.026	.469	.471

TABLE II. - EVAPORATION OF Na_2MoO_4-MoO_3 MELT AT 900 °C

X_{MoO_3}	Rate of evaporation, mg/hr
0	0.024
0.1	0.031
0.2	0.075
0.4	0.51
0.5	0.75
0.6	3.6
0.65	6.6
0.7	12.0
0.8	34.0
0.9	101.19
1.0	320.0

TABLE III.

[Number of millimoles (mM) of Na_2SO_4, Na_2MoO_4, and MoO_3 at different times for corrosion of U-700, coated with 0.7 ($\pm$10 percent) mg/cm^2 Na_2SO_4, and oxidized in O_2 plus 0.108 percent SO_2-SO_3 at 950 °C.]

Time, hr	$\eta_{Na_2SO_4}$	$\eta_{Na_2MoO_4}$	η_{MoO_3}
5 (induction period)	0.019	------	------
46.5	.0057	0.0118	0.0152
50	.0056	.0174	.0086
68	.0021	.0129	.0101
96	.0032	.0158	.0062

TABLE IV.

[Mol fractions of Na_2SO_4, MoO_3 and Na_2MoO_4 in the melt as a function of SO_2 content of the atmosphere.]

SO_2 content	Time, hr	$X_{Na_2SO_4}$	$X_{Na_2MoO_4}$	X_{MoO_3}
105 ppm	30	0.032	0.469	0.471
0.108%	46.5	.174	.362	.464
0.24%	65	.642	.245	.113
1%	80	1	-----	-----
2%	80	1	-----	-----

TABLE V. - RESULTS OF THE CHEMICAL ANALYSIS FOR THE CORROSION OF U-700 IN THE BURNER RIG

Na, wppm	Time, hr	Total Na_2SO_4, mg	Na_2SO_4 per unit surface area, mg/cm^2	Total Na_2CrO_4, mg	Total Na_2MoO_4, mg	Total MoO_3, mg
1	8	0.858	0.110	-----	-----	-----
	23	1.037	.133	-----	-----	-----
	44	1.445	.186	-----	-----	-----
	60	2.524	.325	-----	-----	-----
	80	4.31	.556	1.9	0.309	-----
	100	6.72	.867	2.01	.815	-----
3	10	2.272	.293	.348	-----	-----
	16	2.27	.292	.155	-----	-----
	25	2.54	.327	.189	-----	-----
	28	2.29	.295	.233	-----	-----
	50	2.26	.291	.264	-----	-----
	70.5	24.7	3.18	2.883	8.446	-----
	79	31.2	4.02	3.17	9.012	-----

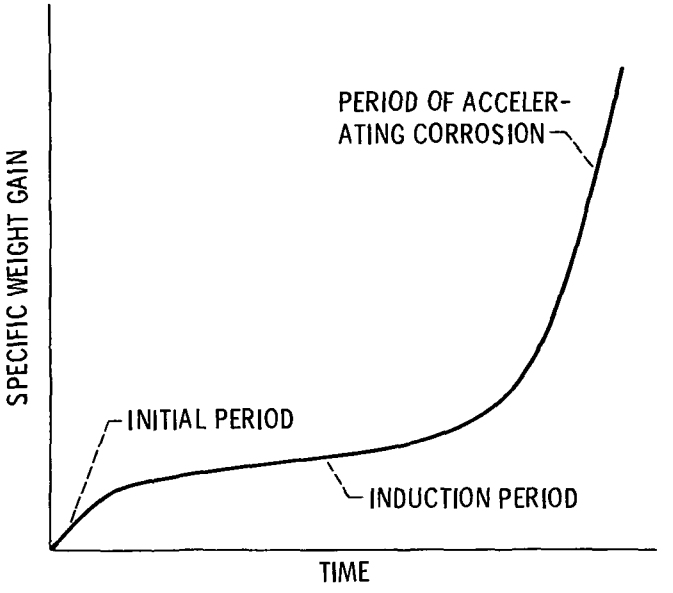

Figure 1. - Schematics of the hot corrosion kinetics in 1 atmosphere O_2 for U-700.

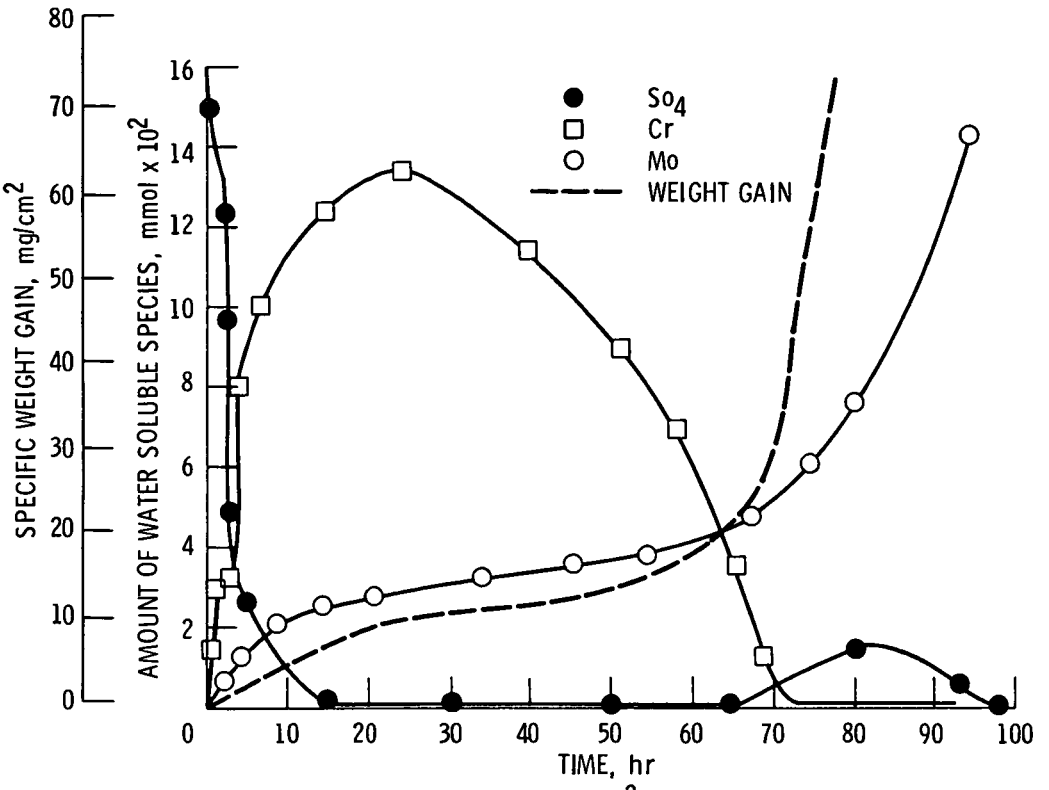

(a) 3.5 mg/cm^2 Na_2SO_4.

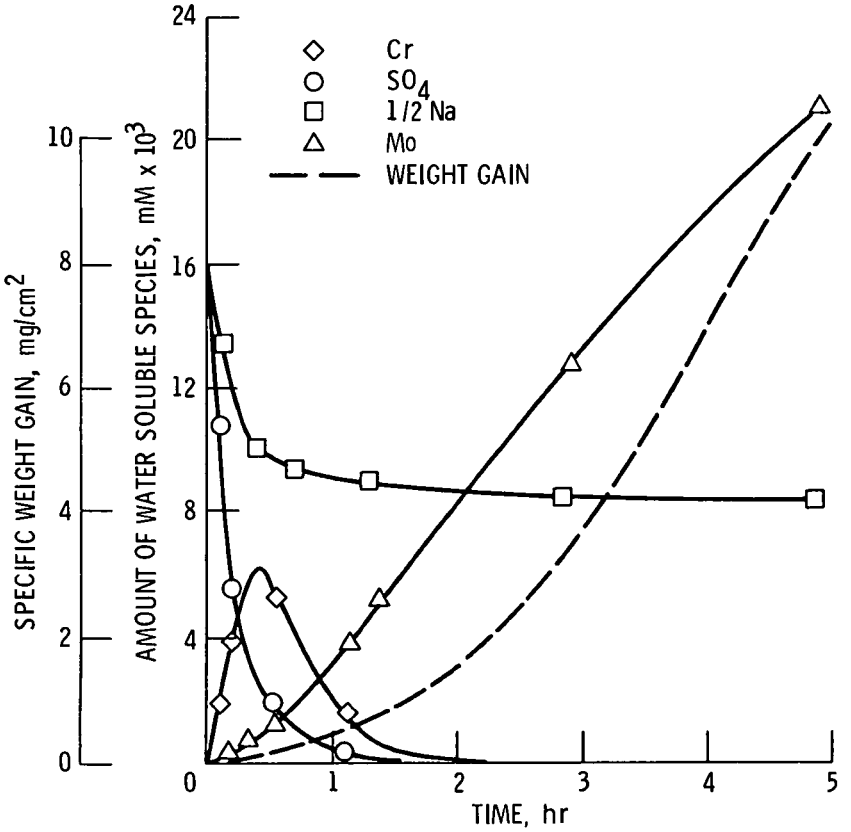

(b) 0.5 mg/cm^2 Na_2SO_4.

Figure 2. - Amount of water soluble species and the weight gain as a function of time for the corrosion of U-700 in 1 atmosphere O_2 at 950 ^{0}C.

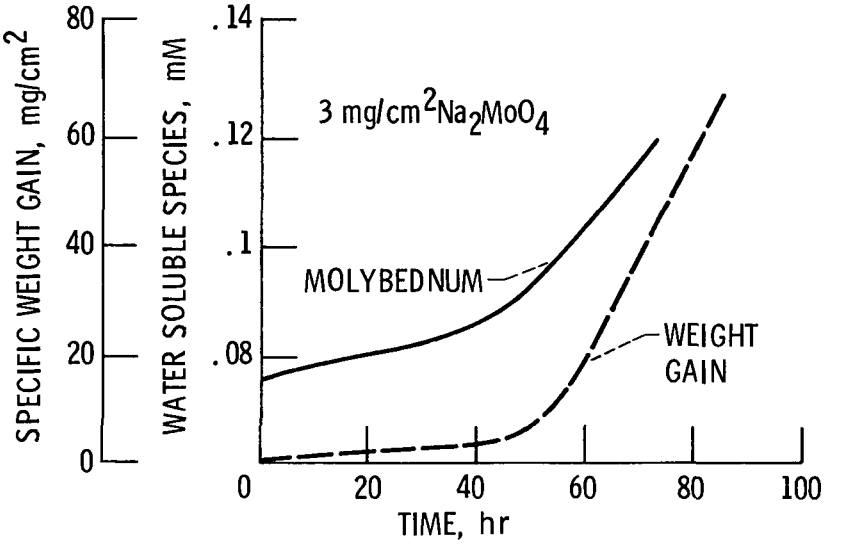

Figure 3. - Amount of water soluble species and the weight gain as a function of time for the corrosion of U-700, coated with 3 mg/cm^2 Na_2MoO_4 and oxidized in 1 atmosphere O_2 at 950 ^{0}C.

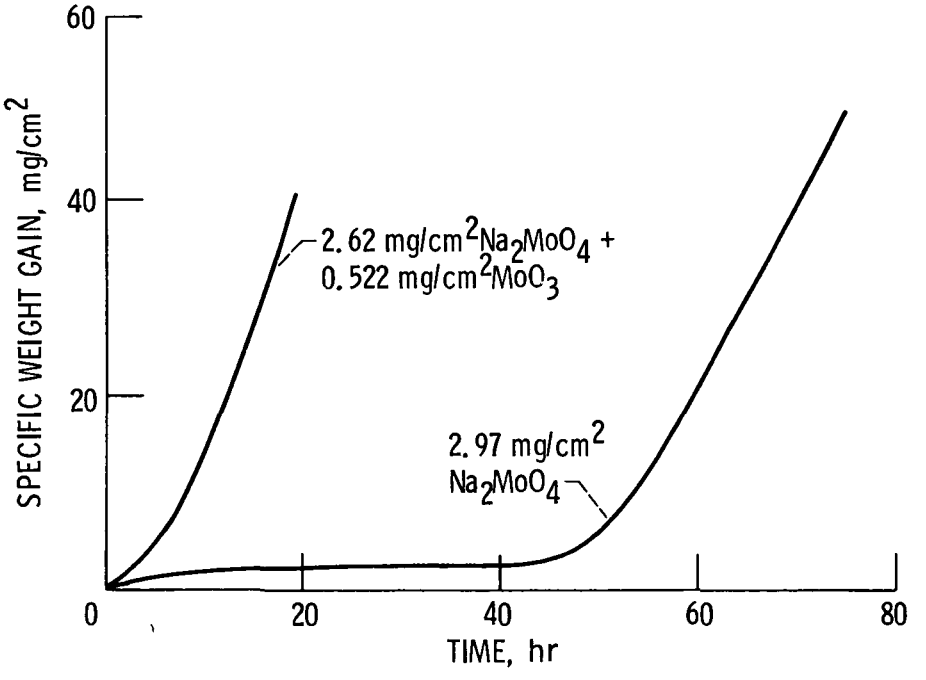

Figure 4. - A comparison of the corrosion kinetics for U-700, coated with Na_2MoO_4 and $Na_2MoO_4 + MoO_3$, and oxidized in 1 atmosphere O_2 at 950 ^{0}C.

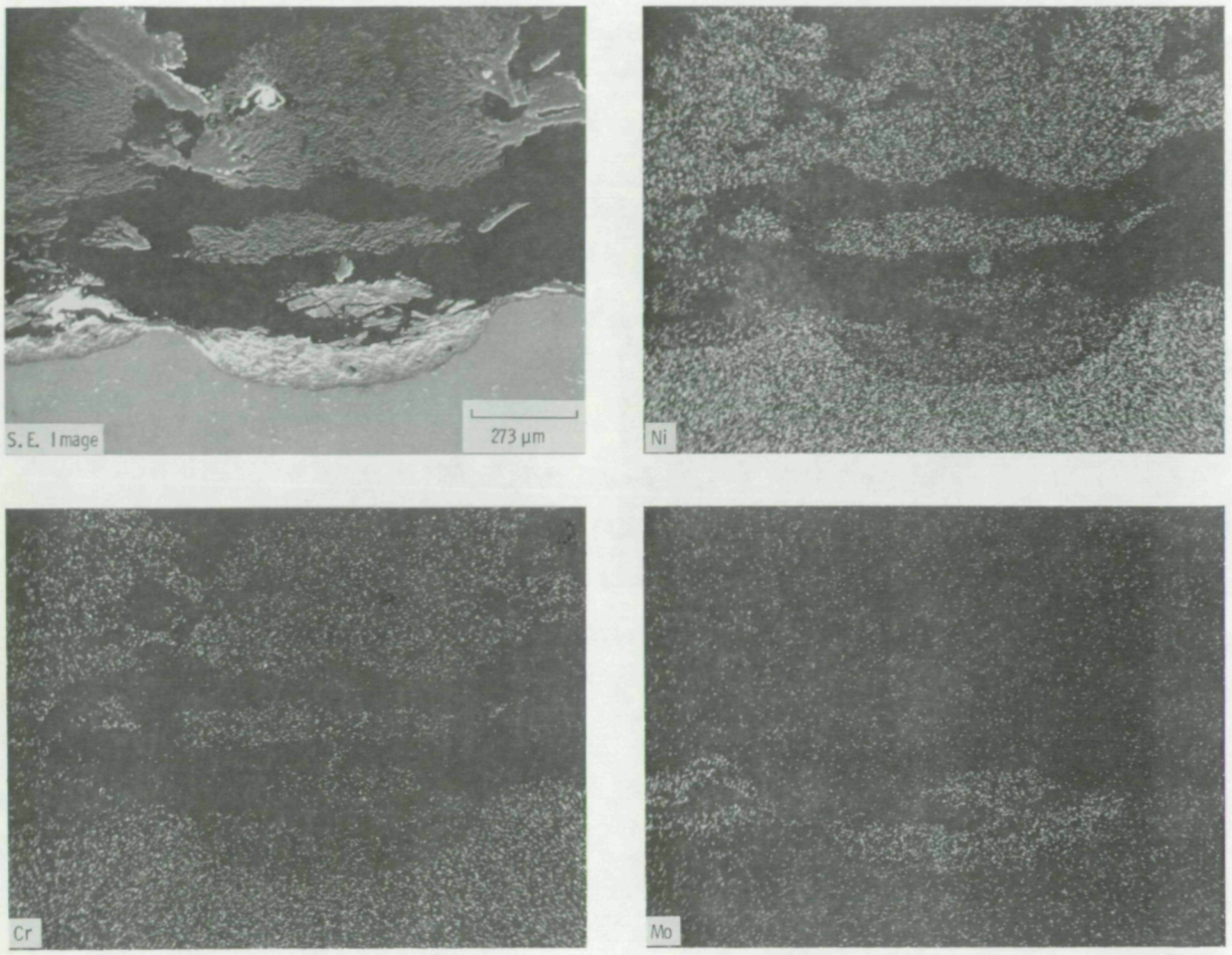

Figure 5. - Typical scale morphology for the corrosion of U-700 by the Na_2MoO_4 - MoO_3 melt.

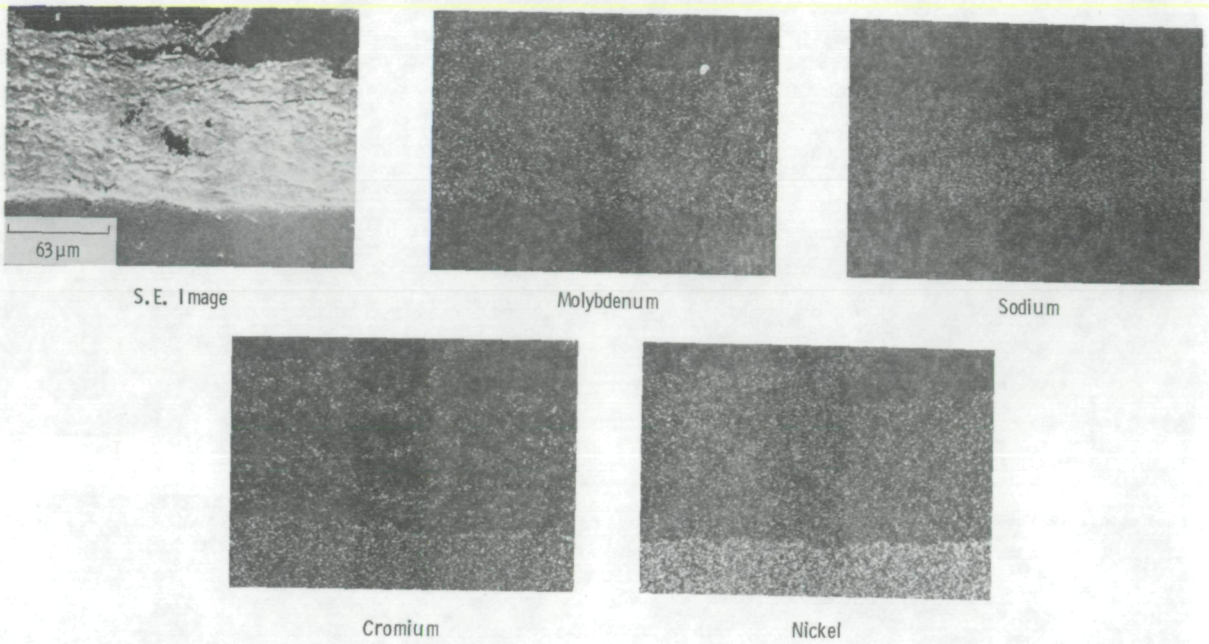

Figure 6. - Details of the pit in figure 5.

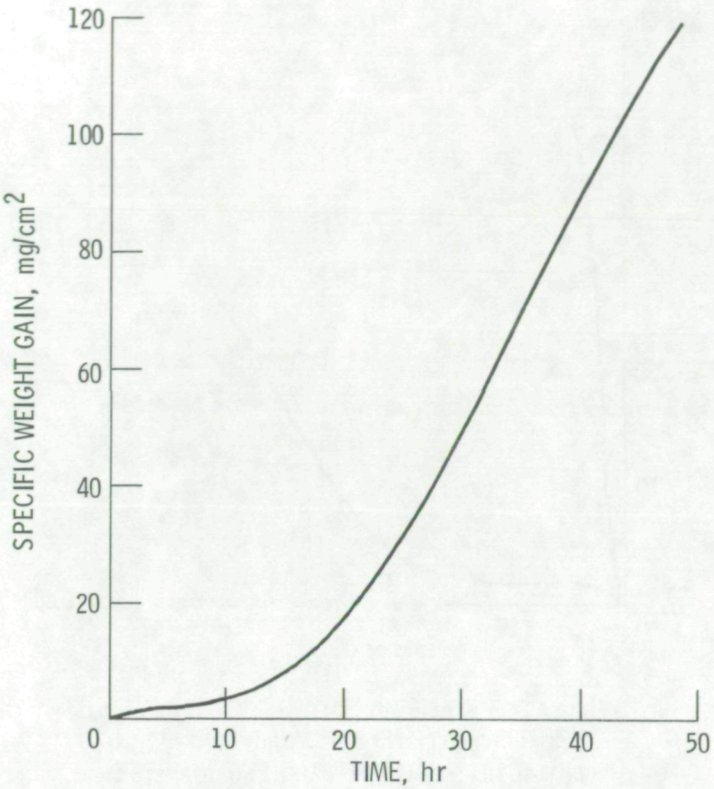

Figure 7. - Kinetics of corrosion for U-700, coated with 0.7 mg/cm^2 Na_2SO_4, and oxidized in O_2 plus 0.108 % SO_2 - SO_3 at 950 ^{0}C.

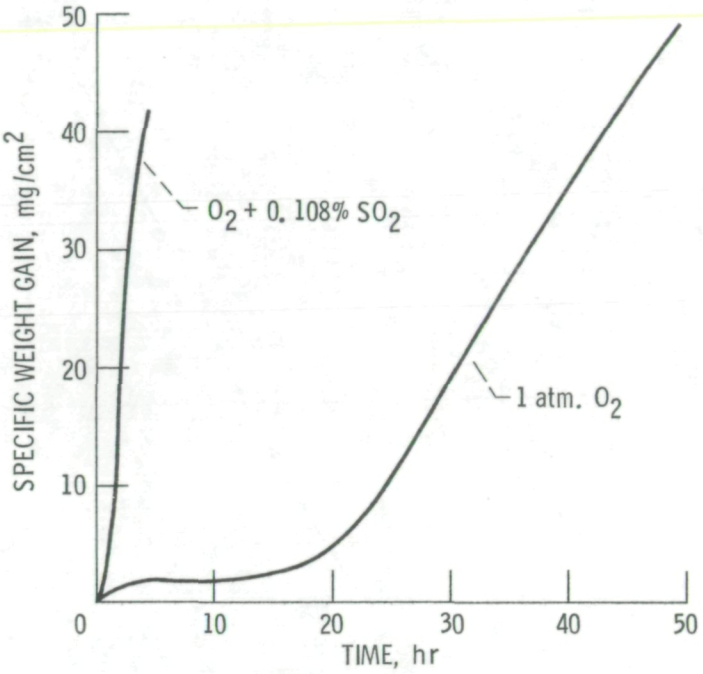

Figure 8. - Kinetics of corrosion for U-700, coated with 1.5 mg/cm^2 Na_2MoO_4, and oxidized in O_2 plus 0.108 % SO_2 - SO_3 and 1 atmosphere O_2 at 950 ^{0}C.

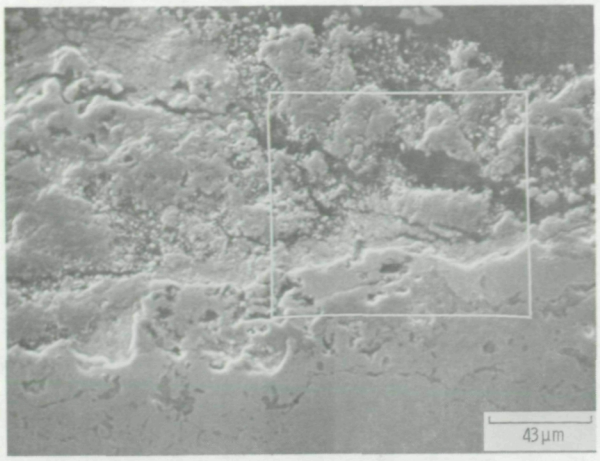

(a) Overall cross section.

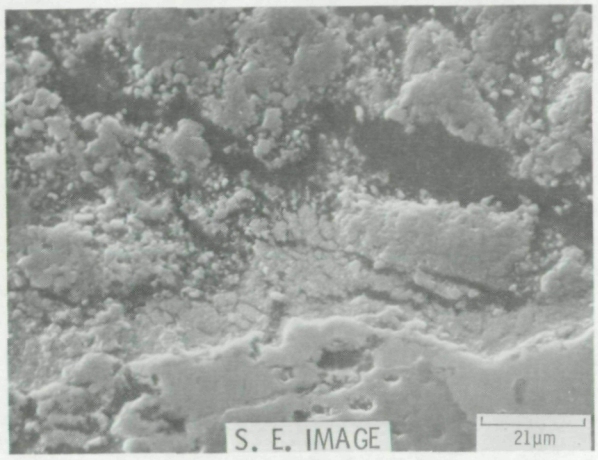

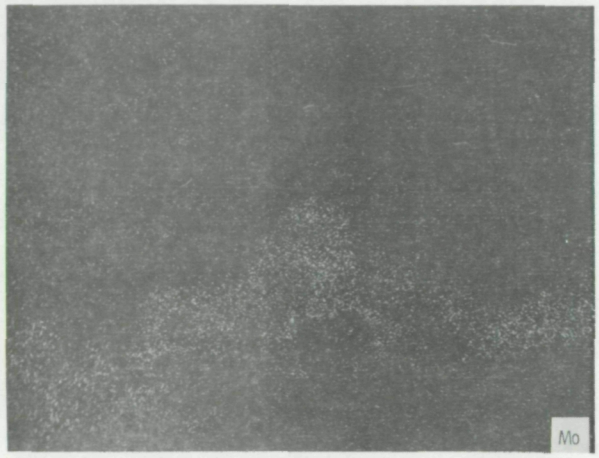

(b) Magnified view of the enclosed area in (a) and the molybdenum x-ray map.

Figure 9. - Typical scale morphology during the period of catastrophic corrosion for corrosion in O_2 plus 0.108 percent SO_2-SO_3 atmosphere.

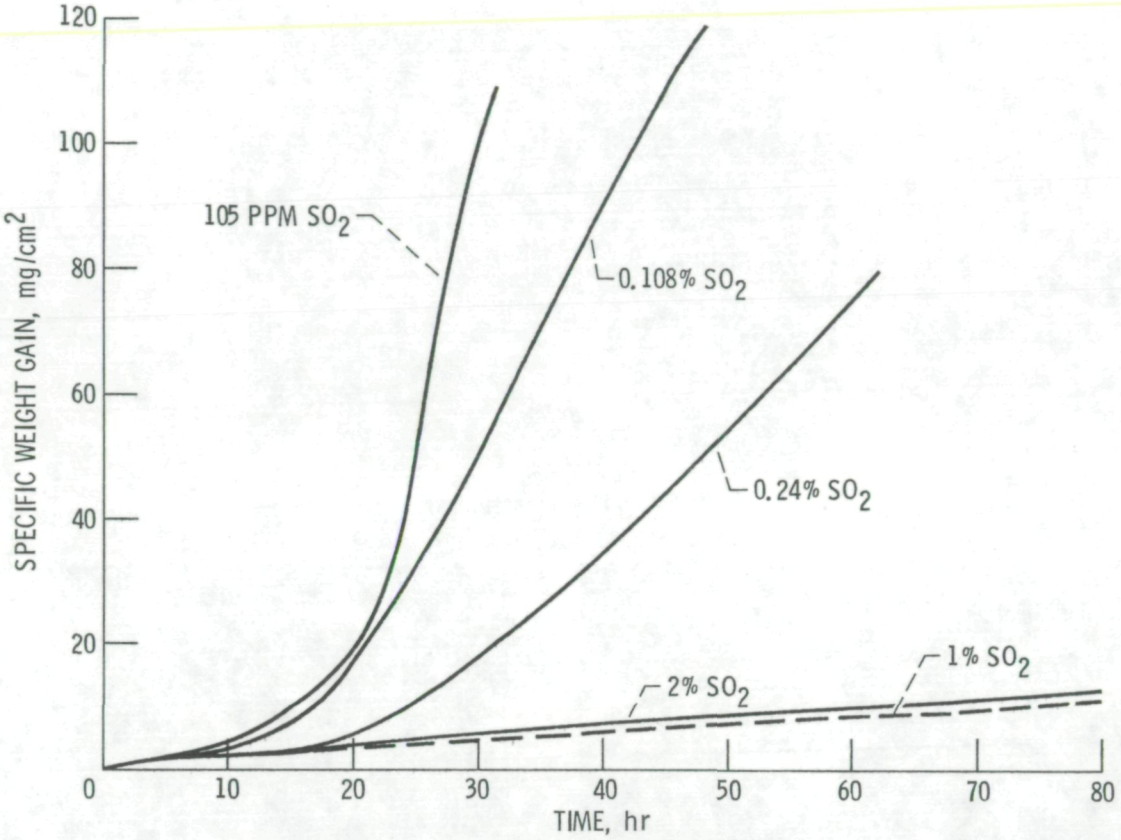

Figure 10. - Effect of $SO_2 + SO_3$ concentration on the corrosion kinetics for U-700, coated with 0.7 mg/cm^2 Na_2SO_4, and oxidized at 950 ^{o}C.

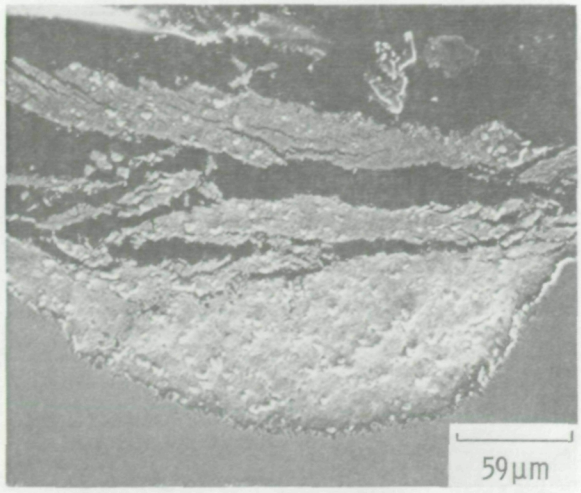

Figure 11. - Scale morphology for U-700, coated wtih about 0.7 mg/cm^2 Na_2SO_4, and oxidized in O_2 plus 105ppm SO_2-SO_3 for 30 hr at 950^0 C.

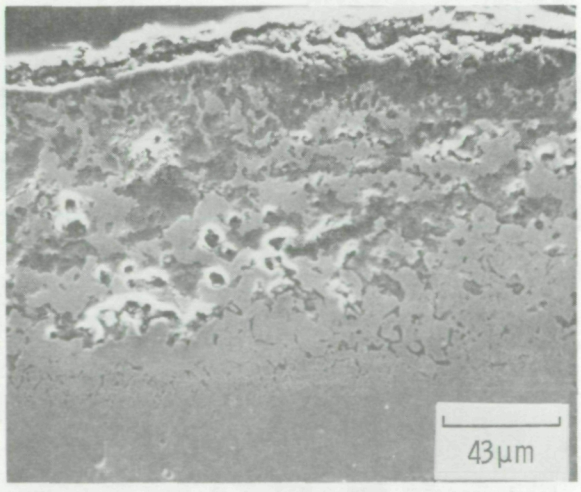

Figure 12. - Scale morphology for U-700, coated with about 0.7 mg/cm^2 Na_2SO_4, and oxidized in O_2 plus 1% SO_2-SO_3 for 60 hr at 950^0 C.

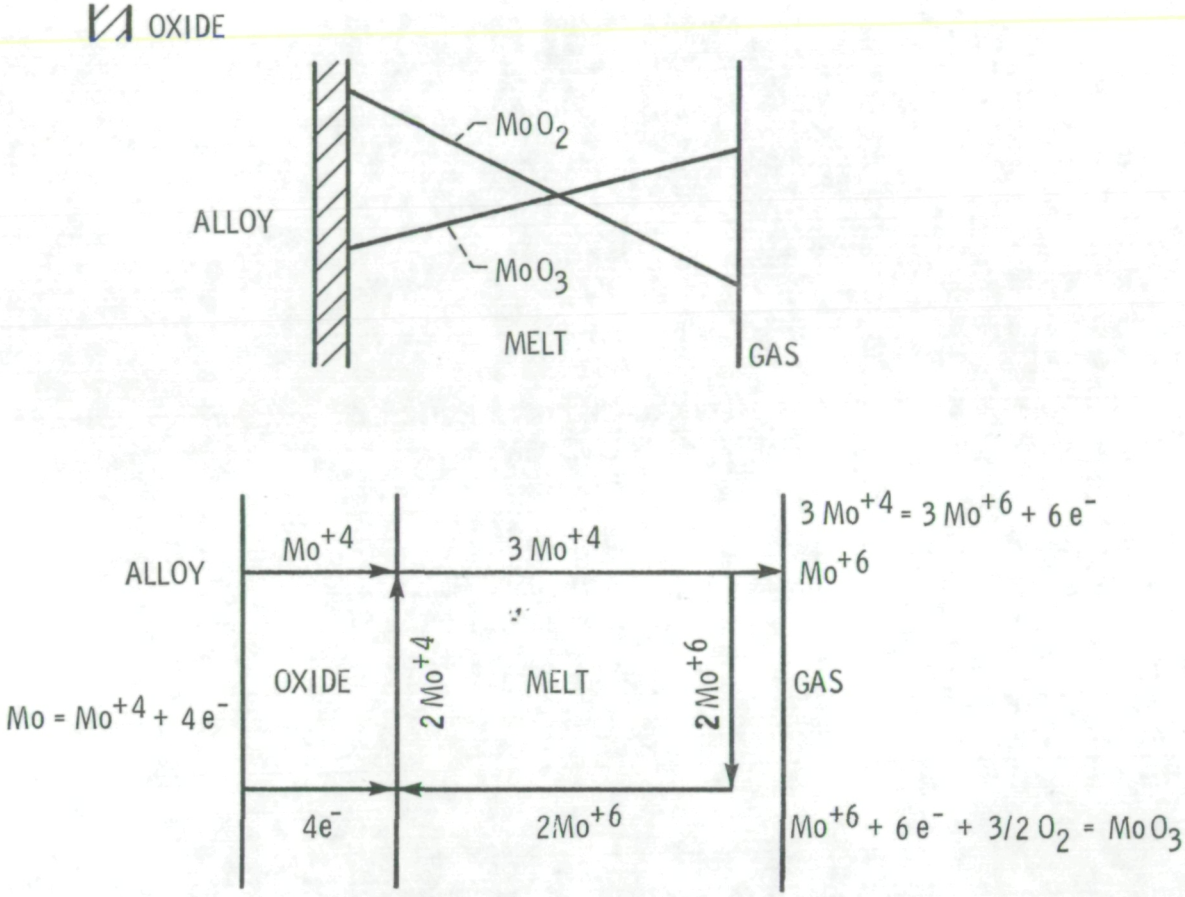

Figure 13. - Schematics of the mechanism for the formation of MoO_3.

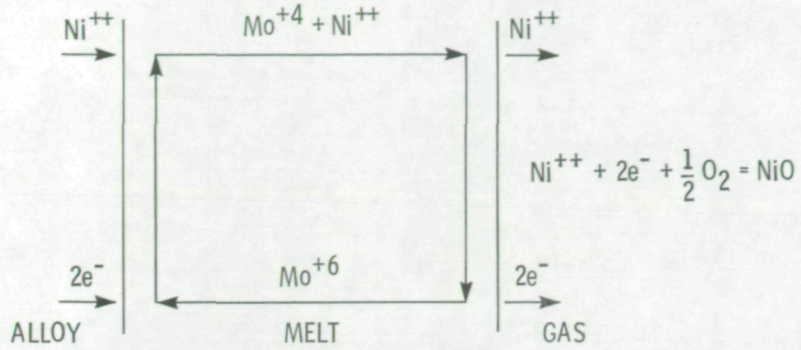

Figure 14. - Schematics of the mechanism of corrosion beneath the Na_2MoO_4 - MoO_3 melt.

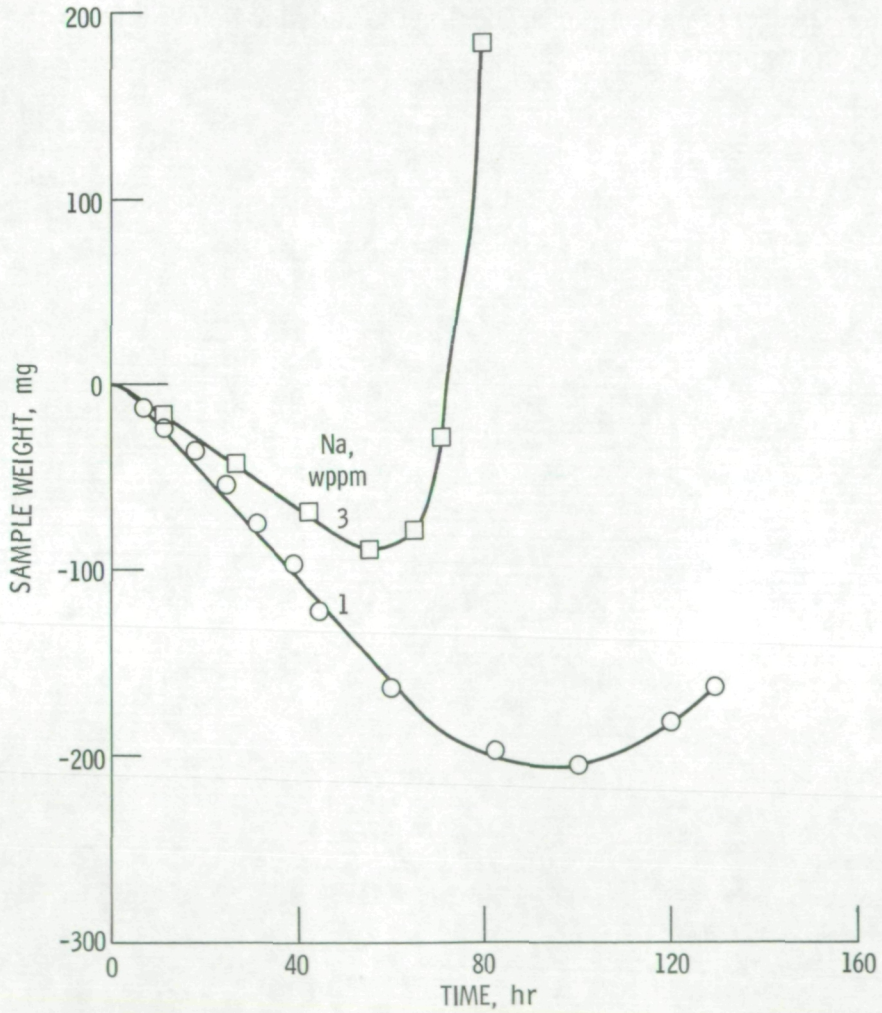

Figure 15. - Weight change data as a function of time for corrosion of U-700 in the burner rig at 900 ^{0}C.

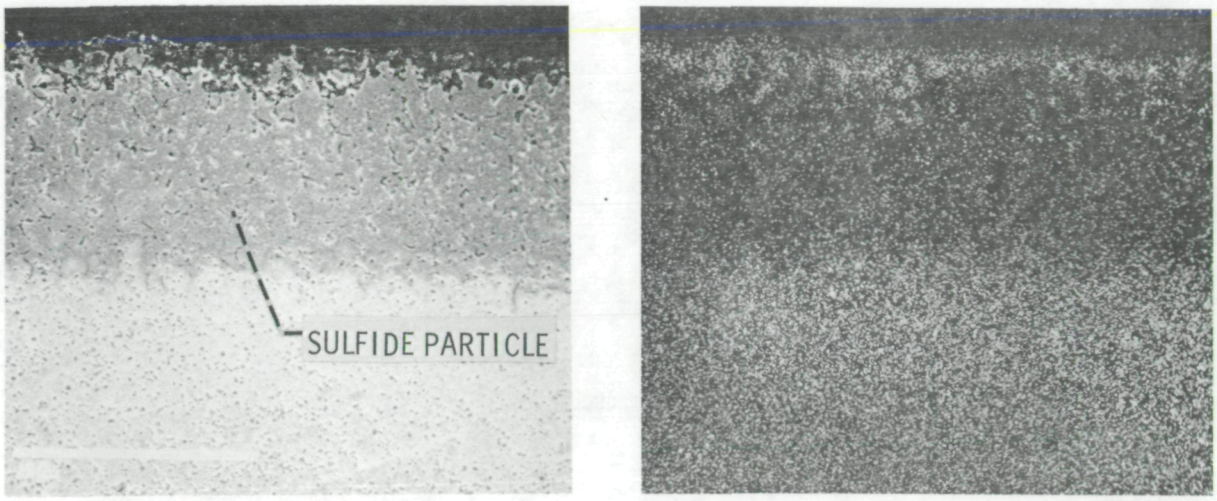

S. E. Image

Cr x-ray map

Figure 16. - Typical scale morphology during the period of weight loss for the corrosion of U-700 in the burner rig.

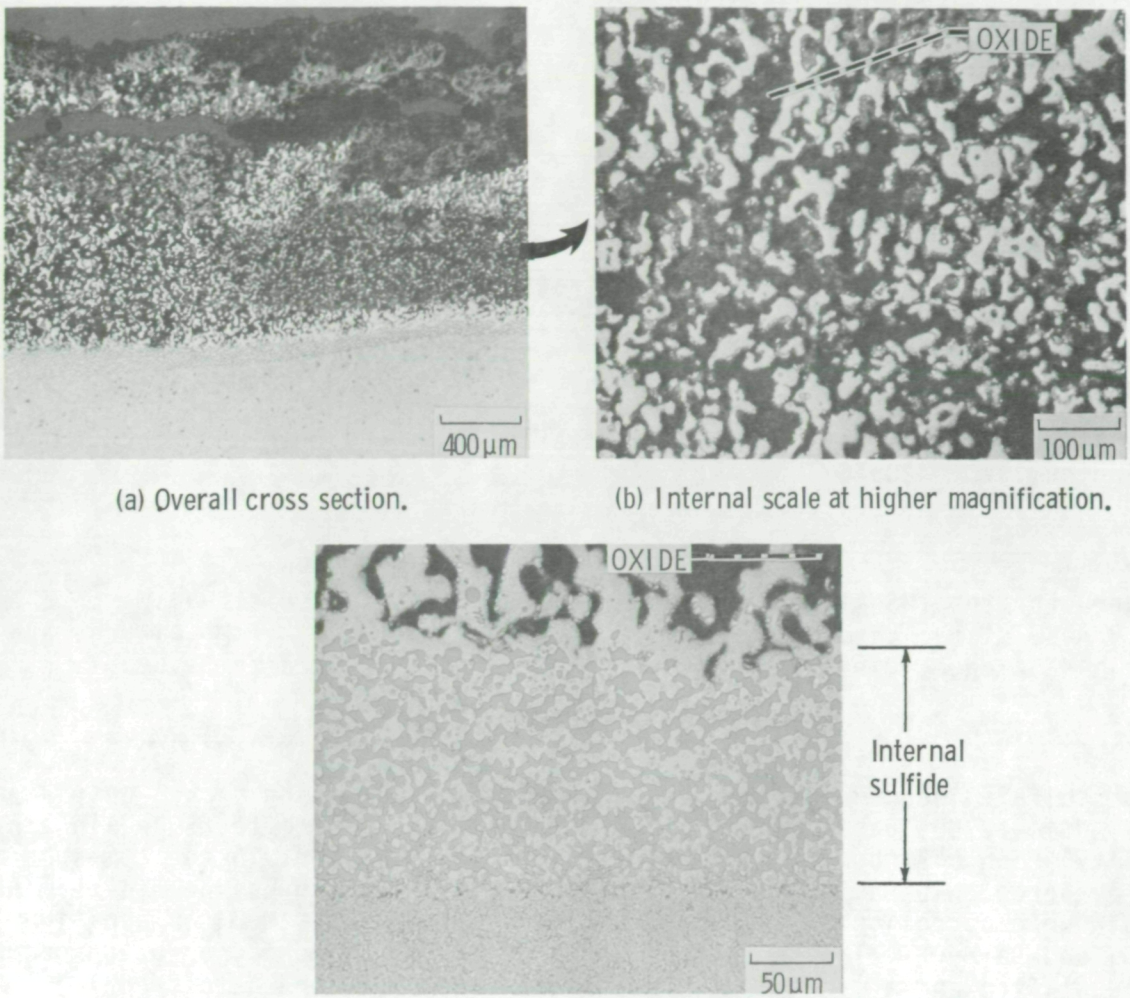

(a) Overall cross section.

(b) Internal scale at higher magnification.

(c) Scale-metal interface showing large sulfide network.

Figure 17. - Scale morphology during the period of weight gain for the corrosion of U-700 in 3 wppm Na in the burner rig at 900° C.

1. Report No.	2. Government Accession No.	3. Recipient's Catalog No.
NASA TM-87235		

4. Title and Subtitle	5. Report Date
Role of Molybdenum in the Na_2SO_4 Induced Corrosion of Superalloys at High Temperature	6. Performing Organization Code: 505-63-11

7. Author(s)	8. Performing Organization Report No.
A.K. Misra	E-2905
	10. Work Unit No.

9. Performing Organization Name and Address	11. Contract or Grant No.
National Aeronautics and Space Administration Lewis Research Center Cleveland, Ohio 44135	13. Type of Report and Period Covered: Technical Memorandum
12. Sponsoring Agency Name and Address	14. Sponsoring Agency Code
National Aeronautics and Space Administration Washington, D.C. 20546	

15. Supplementary Notes

Prepared for the TMS-AIME Annual Meeting, New Orleans, Louisiana, March 2-6, 1986. A.K. Misra, Case Western Reserve University, Dept. of Metallurgy and Materials Science, Cleveland, Ohio and NASA Resident Research Associate.

16. Abstract

Sodium sulfate induced corrosion of a molybdenum containing nickel-base superalloy, Udimet 700, have been studied in laboratory furnace tests and in a high velocity (Mach 0.3) burner rig. The effect of SO_2 content in the atmosphere on the corrosion behavior in the laboratory furnace tests has been determined. Catastrophic corrosion occurs only when the melt contains MoO_3 in addition to Na_2SO_4 and Na_2MoO_4. The conditions under which catastrophic corrosion occurs are identified and a mechanism is described to explain the catastrophic corrosion.

17. Key Words (Suggested by Author(s))	18. Distribution Statement
Superalloys Molybdenum Hot corrosion	Unclassified - unlimited STAR Category 26

19. Security Classif. (of this report)	20. Security Classif. (of this page)	21. No. of pages	22. Price*
Unclassified	Unclassified		

*For sale by the National Technical Information Service, Springfield, Virginia 22161

National Aeronautics and
Space Administration

Lewis Research Center
Cleveland, Ohio 44135

SECOND CLASS MAIL

ADDRESS CORRECTION REQUESTED

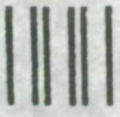

Official Business
Penalty for Private Use $300

Postage and Fees Paid
National Aeronautics and
Space Administration
NASA-451

NASA